Journal of Power Sources 260 (2014) 317–325

Contents lists available at ScienceDirect

Journal of Power Sources

journal homepage: www.elsevier.com/locate/jpowsour

Preparation and characterization of high performance sulfonated poly(*p*-phenylene-*co*-aryl ether ketone) membranes for direct methanol fuel cells

Qingyi He [a,b], Jifu Zheng [a,1], Suobo Zhang [a,*]

[a] Key Laboratory of Polymer Ecomaterials, Changchun Institute of Applied Chemistry, Chinese Academy of Sciences, Changchun 130022, China
[b] Graduate School of Chinese Academy of Sciences, Beijing 100039, China

HIGHLIGHTS

- Sulfonated poly(*p*-phenylene-*co*-aryl ether ketone)s were prepared as PEM materials.
- SPP-*co*-PAEK CN *x* membranes displayed good oxidative stability, low methanol permeability and swelling ratio.
- SPP-*co*-PAEK CN 1.86 membrane exhibited comparable cell performance with Nafion®117.

GRAPHICAL ABSTRACT

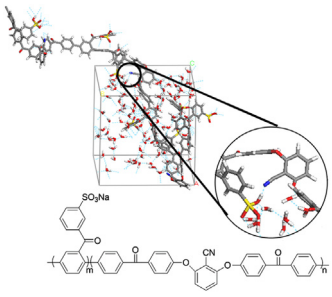

ARTICLE INFO

Article history:
Received 31 December 2013
Received in revised form
23 February 2014
Accepted 10 March 2014
Available online 18 March 2014

Keywords:
Sulfonated poly(*p*-phenylene-*co*-aryl ether ketone)s
Oxidative stability
Cell performance
Glass-transition temperature
Proton conductivity

ABSTRACT

A series of sulfonated poly(*p*-phenylene-*co*-aryl ether ketone)s (SPP-*co*-PAEK) have been designed as membrane materials for direct methanol fuel cell (DMFC) applications. The materials for such membranes have been prepared via the nickel (0) catalyzed coupling copolymerization of 2,5-dichloro-3-sulfobenzophenone and 2,6-bis(4-(4-chlorobenzoyl)phenoxy)benzonitrile. The SPP-*co*-PAEK membranes show the desired characteristics such as excellent thermal and mechanical properties, good oxidative stability, low methanol permeability and well-defined micro-phase separation. With an ion exchange capacity (IEC) ranging from 1.90 to 2.59 mequiv g^{-1}, these membranes display comparable proton conductivity (0.085–0.170 S cm^{-1}) to Nafion®117 when fully hydrated at 80 °C. In addition, the passive direct methanol fuel cell with SPP-*co*-PAEK CN 1.86 (IEC = 1.90 mequiv g^{-1}) membrane presents a maximum power density of 24.5 mW cm^{-2} at 25 °C, which is comparable to the value of Nafion®117 (24.3 mW cm^{-2}).

1. Introduction

Proton exchange membrane fuel cells (PEMFCs) have attracted a lot of attention in recent times as clean energy-conversion devices for stationary, transportation and portable applications due to their high energy-conversion efficiency and low emissions [1]. Proton exchange membrane (PEM) is one of the key components of PEMFCs and its properties have a great effect on the cell

* Corresponding author. Tel.: +86 431 85262118; fax: +86 431 85685653.
E-mail addresses: jfzheng@ciac.ac.cn, sbzhang@ciac.jl.cn (J. Zheng), sbzhang@ciac.ac.cn (S. Zhang).
[1] Tel./fax: +86 431 85262117.

http://dx.doi.org/10.1016/j.jpowsour.2014.03.028
0378-7753/

performance [2,3]. The perfluorosulfonic acid polymer membranes, such as Nafion®, are mostly used PEMs because of their excellent mechanical property, good chemical and thermal stability, and good endurance under fuel cell conditions. However, their inherent drawbacks which include high cost, high methanol permeability, and low operating temperature have limited their further development for applications in PEMFCs [4]. Therefore, the investigation of promising new membranes is an area of extensive research, with sulfonated aromatic polymers (SAPs) being the most actively studied of them. As potential alternatives to Nafion® in PEMFCs, these new membranes present ideal characteristics, such as high proton conductivity and low methanol permeability [5–10]. Among them, sulfonated polyphenylenes (SPPs) and their derivatives are of interest because of their excellent thermal and chemical stabilities [11–20] and ease of synthesis via a nickel (0) catalyzed coupling reaction. For example, McGrath et al. reported the formation of SPPs by nickel-catalyzed coupling polymerization of 2, 5-dichloro-4′-substituted benzophenones, followed by post-sulfonation to introduce sulfonic acid groups [18]. Ohira et al. prepared a series of SPPs containing aliphatic alkyl pendent side chains to improve their solubility and film-forming ability [12]. More recently, Wang and co-workers modified the SPPs by introducing an ether linkage and perfluoroisopropyl group into polymer chains to enhance their solubility [20]. Quite recently, Rikukawa and co-workers reported a series of hydrophilic-hydrophobic block SPPs with controlled block lengths using a catalyst-transfer polycondensation method [13].

In our previous reports, we have discussed about the development of a series of SPPs and their derivatives by introducing dichlorobenzophenone and naphathalimide segments into the polymer backbones [16,17]. These polymers showed good solubility and film-forming ability, and their corresponding membranes displayed good oxidative stability and comparable proton conductivity to Nafion®. But unfortunately because of their rigid chemical structure these membranes had a high glass-transition temperature (Tg), and hence they could barely be used to prepare membrane-electrode assembly (MEA). Hot-pressing method is frequently used to make MEAs, and high glass-transition temperatures of PEMs can sometimes result in poor adhesion between the electrode and membrane which can have adverse effects on the cell performance [2,21]. Based on this consideration, structural modification of SPPs is an area of further development.

Generally, introducing ether linkages into the polymer backbone can lower the Tg of the polymer, especially the ionomers containing *meta* ether linkages have lower glass-transition temperatures than with *para* ether linkages [22]. Therefore, we have designed and synthesized two novel aromatic dichloride monomer 2,6-bis(4-(4-chlorobenzoyl)phenoxy)benzene (1) and 2,6-bis(4-(4-chlorobenzoyl)phenoxy)benzonitrile (2) containing *meta* ether linkages and carbonyl groups, with monomer **2** containing an extra cyano group. The cyano-containing polymers usually have strong interactions with the matrix which is thought to be favorable when they are used as PEMs. These two new monomeric hydrophobic units were then individually used to copolymerize with 2,5-dichloro-3-sulfobenzophenone via a nickel (0) catalyzed coupling method for preparing novel SPPs. Finally, a series of sulfonated poly(*p*-phenylene-*co*-aryl ether ketone)s (SPP-*co*-PAEK) membranes, were prepared. The glass-transition temperature of these membranes was determined by DMA and membrane-electrode assembly was prepared by the hot-pressing method. In this report, we have investigated the water uptake, oxidative stability, methanol permeability, proton conductivity and cell performance of this new series of PEMs and compared with the reported SPPs and Nafion® as shown in Fig. 1. Based on the study it was found that the SPP-*co*-PAEK CN 1.86 membrane exhibited comparable single-cell performance with that of Nafion®117 and the best oxidative stability among all the obtained SPP-*co*-PAEK membranes.

2. Experimental section

2.1. Materials

N,*N*-Dimethylacetamide (DMAc) was dried over CaH_2, distilled under reduced pressure, and stored over 4 Å molecular sieves. Reagent grade anhydrous $NiBr_2$ was dried at 220 °C under vacuum. Triphenylphosphine (PPh_3) was recrystallized from hexane. Zinc dust was stirred with acetic acid, filtered, washed thoroughly with diethyl ether, and dried under vacuum. All other reagents were used as received. Resorcinol was purchased from Beijing chemical agent company. 2,5-Dichlorobenzophenone and 4-chloro,4′-hydroxydibenzophenone were purchased from Energy agent company (ShangHai, China). 2,6-Difluorobenzonitrile was purchased from Aldrich. 2,5-Dichloro-3-sulfobenzophenone (SBJT) was prepared by sulfonation of 2,5-dichlorobenzophenone according to previously described procedure [17]. 4-Chloro,4′-fluorobenzophenone was prepared according to a reported method [23].

2.2. Synthesis of 2,6-bis(4-(4-chlorobenzoyl)phenoxy)benzene **1**

4-Chloro,4′-fluorobenzophenone (4.69 g, 20 mmol), resorcinol (1.10 g, 10 mmol), and potassium carbonate (3.04 g, 22 mmol) were dissolved in 30 ml DMAc. The reaction mixture was stirred at 80 °C for 12 h in the atmosphere of nitrogen. Then the mixture was cooled and poured into 200 ml water. The white precipitate was filtered and dried in vacuo yield to 4.96 g (92.0%).

^{1}H NMR (300 MHz, DMSO; ppm): δ 7.80 (d, 4H, $J = 9.0$ Hz), 7.74 (d, 4H, $J = 9.0$ Hz), 7.62 (d, 4H, $J = 9.0$ Hz), 7.54 (t, 1H, $J = 9.0$ Hz), 7.18 (d, 4H, $J = 9.0$ Hz), 7.02 (dd, 2H, $J = 9.0$ Hz, $J = 3.0$ Hz), 6.96 (d, 1H, $J = 3.0$ Hz). ^{13}C NMR (75 MHz, DMSO; ppm): δ 193.2, 166.4, 163.1, 137.6, 135.6, 133.2, 133.1, 132.6, 132.5, 131.4, 128.7, 115.9, 115.4. ESMS: 539.2 $(M + H)^+$.

2.3. Synthesis of 2,6-bis(4-(4-chlorobenzoyl)phenoxy)benzonitrile **2**

4-Chloro,4′-hydroxydibenzophenone (4.65 g, 20 mmol), 2,6-difluorocyanophenyl (1.39 g, 10 mmol), and potassium carbonate (3.04 g, 22 mmol) were dissolved in 30 ml DMAc. The following procedure is the same as the monomer **1** prepared. A white power was achieved and dried in vacuo yield to 5.13 g (90.9%).

^{1}H NMR (300 MHz, DMSO; ppm): δ 7.87 (d, 4H, $J = 9.0$ Hz), 7.78 (d, 4H, $J = 9.0$ Hz), 7.71 (d, 1H, $J = 9.0$ Hz), 7.65 (d, 4H, $J = 9.0$ Hz), 7.37 (d, 4H, $J = 9.0$ Hz), 7.01 (d, 2H, $J = 9.0$ Hz). ^{13}C NMR (75 MHz, DMSO; ppm): δ 194.1, 159.8, 158.4, 139.0, 135.7, 134.6, 133.6, 132.3, 131.3, 128.8, 118.9, 112.6, 112.1, 97.5. ESMS: 564.2 $(M + H)^+$.

2.4. Synthesis of SPP-co-PAEK copolymers

The nomenclature of SPP-*co*-PAEK copolymers achieved in this study is SPP-*co*-PAEK CN *x* or SPP-*co*-PAEK MO *x*, where *x* refers to the molar ratio of SBJT to **1** or **2**. In addition, SPP-*co*-PAEK MO *x* means that the copolymers were prepared from SBJT and **1**, while SPP-*co*-PAEK CN *x* means that the copolymers were prepared from SBJT and **2**. A typical procedure for the preparation of SPP-*co*-PAEK CN 2.33 has been described herein.

$NiBr_2$ (0.156 g, 0.71 mmol), PPh_3 (1.30 g, 5.00 mmol), and zinc dust (2.56 g, 40.00 mmol) were placed in a 100 ml three-necked round-bottomed flask. The flask was evacuated and filled with nitrogen three times. Dry DMAc (20 ml) was added via syringe. The

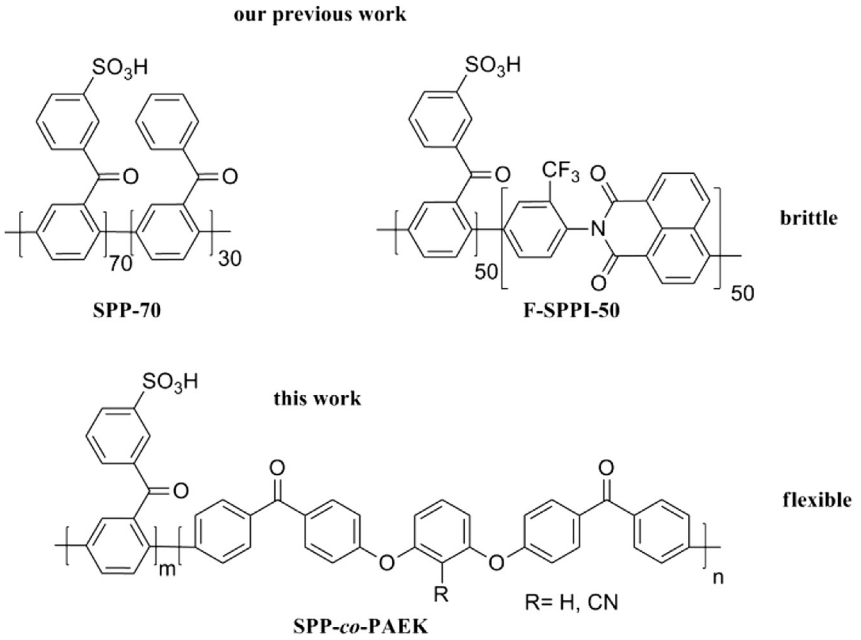

Fig. 1. Structures of SPP-70 and F-SPPI-50 we reported before and SPP-*co*-PAEK copolymers obtained in this work.

mixture was stirred at 80 °C and then its color changed to red brown in 20 min. Then the monomer **2** (3.00 mmol) and SBJT (7.00 mmol) were added into the flask. The reaction was performed at 80 °C for 12 h. The resulting viscous mixture was diluted with 20 ml of DMAc, and then poured into 300 ml of 10%wt HCl solution. The fiber-like polymer was collected by filtration, washed with diethyl ether, dried under vacuum (yield: 97.0%).

2.5. Membrane preparation

The polymers obtained were dissolved in DMAc to form a 5–8 wt. % solution which was then filtered and cast on a glass plate. The solvent was evaporated in an oven at 60 °C for 8 h and then at 150 °C under vacuum for 12 h. Next, the membranes were immersed into 1 N sulfuric acid at room temperature for 24 h. Finally, the membranes were thoroughly washed with deionized water and dried under vacuum at 120 °C for 12 h. The thickness of the resulting membranes was in the range of 40–60 μm.

2.6. Measurements

^{1}H NMR spectra were measured on an AV 300 spectrometer. FT-IR spectra were obtained with a Bio-Rad Digilab Division FTS-80 FT-IR spectrometer. The thermogravimetric analyses (TGA) were obtained between 50 and 800 °C under nitrogen with a Perkin–Elmer TGA-2 thermogravimetric analyzer at a heating rate of 10 °C min^{-1}. The inherent viscosities were determined at 0.5% concentration of the polymer in DMAc with an Ubbelohde capillary viscometer at 30 ± 0.1 °C. Tensile measurements were conducted with an Instron-1211 at a speed of 1 mm min^{-1} at room temperature and ambient humidity conditions. TEM analysis was performed with slices of Pb^{2+}-stained SPP-*co*-PAEK membranes on JEM-1011. The sample in the protonated form changed into the Pb^{2+} form by immersing the sample on a copper grid in $Pb(OAc)_2$ solution, after which it was thoroughly rinsed with water and dried at room temperature for 24 h.

Water uptake (WU) and dimensional change of the membranes were investigated by immersing the dry samples into water at room temperature for several hours. Water uptake of the membranes was calculated from Equation (1):

$$WU = [(W_w - W_d)/W_d] \times 100 \quad (1)$$

Where W_d and W_w are the weight of dry and corresponding water swollen membranes, respectively.

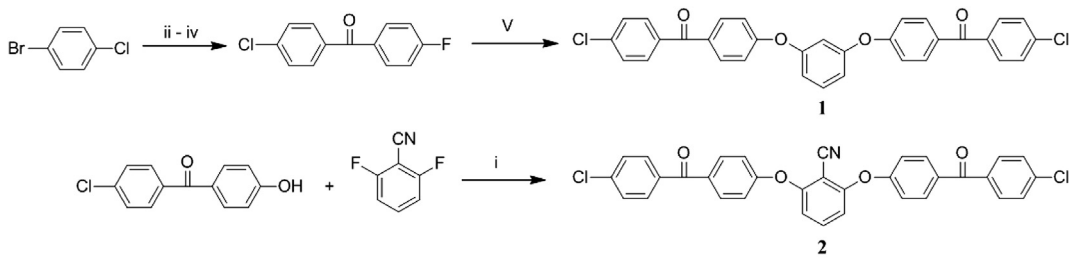

Reagent and conditions: (i) K_2CO_3, DMAC, N_2, 80°C, 6 h. (ii) n-Buli (1.1equiv.), THF. (iii) 4-FC_6H_4CHO (1.05 equiv.), 1h, -78 °C. (iv) I_2 (1.6 equiv.), K_2CO_3 (3.0 equiv.) t-BuOH, 12 h, refulx. (V) K_2CO_3, DMAC, N_2, 80°C, 6 h.

Scheme 1. Syntheses of monomers **1** and **2**.

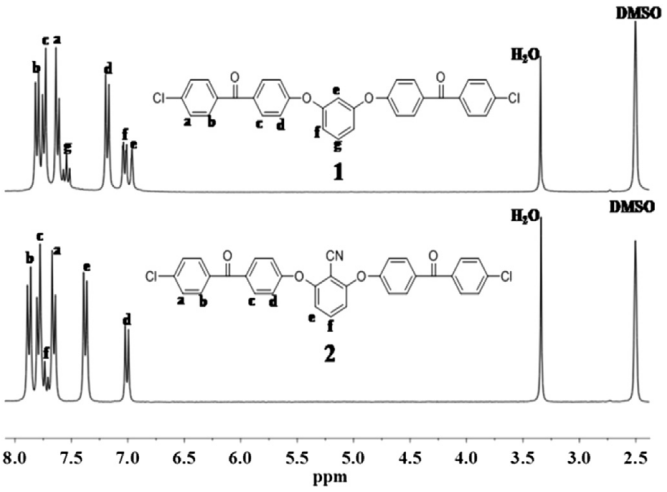

Fig. 2. ^{1}H NMR spectra of monomers **1** and **2**.

Thickness and diameter changes of the membranes were calculated from Equation (2):

$$\Delta T_c = (T - T_s)/T_s$$

$$\Delta L_c = (L - L_s)/L_s \quad (2)$$

Where T_s and L_s are the thickness and diameter of the membrane equilibrated at 70% RH, respectively; T and L refer to those of the membrane immersed in water for 5 h.

Oxidative stability of the membranes was evaluated by measuring the time at which the dissolution process of the membrane starts and thereafter it dissolves completely after immersing them in 30% H_2O_2 containing 30 ppm $FeSO_4$ at 25 °C [16,17]. An accelerated test was also performed for further evaluation of the oxidative stability of these membranes. During the test, the membrane was immersed in Fenton's reagent containing 3% H_2O_2 and 2 ppm $FeSO_4$ at 80 °C for 1 h and the retained weights (RW) of these membranes were recorded.

The proton conductivities of the membranes were evaluated using electrochemical impedance spectra within the temperature range of 30–80 °C (100% relative humidity). The resistance value (R) was measured over the frequency range of 10 Hz–100 KHz by four-point probe AC impedance spectroscopy using an electrode system connected with an impedance/gain-phase analyzer

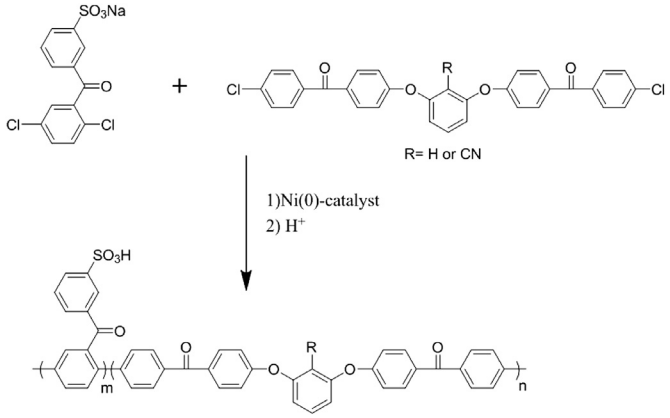

Scheme 2. Syntheses of SPP-*co*-PAEK copolymers.

Table 1
Mechanical properties of SPP-*co*-PAEK membranes.

Sample[a]	η_{red}[b] (dL g^{-1})	Tensile strength (MPa)	Young's modulus (GPa)	Elongation at break (%)
SPP-*co*-PAEK CN 4.00	1.36	15.0	0.20	14.0
SPP-*co*-PAEK CN 2.33	1.23	47.0	0.30	65.0
SPP-*co*-PAEK CN 1.86	1.08	18.4	0.70	35.0
SPP-*co*-PAEK MO 2.33	1.19	26.3	0.28	30.0
SPP-70[c]	1.20	20.2	0.50	12.7
F-SPPI-50[c]	2.35	56.0	1.27	9.0

[a] Samples were dried at ambient conditions for 12 h and tested at 30 °C, and ambient humidity conditions.
[b] Reduced viscosity measured at 0.5 g dL^{-1} in DMAC at 30 °C.
[c] Previously synthesized and added for comparison [16,17].

(Solatron 1260) and an electrochemical interface (Solatron 1287, Farnborough Hampshire, ONR, UK). The membranes with 1 cm^2 in area were sandwiched between two stainless steel blocking electrodes. The membranes were allowed to equilibrate at the desired temperature for 30 min and the measurements were taken every 15 min until the obtained conductivity became constant. Proton conductivity was calculated from Equation (3):

$$\sigma = d/(LWR) \quad (3)$$

Where d is the distance between the two electrodes, and L and W are the thickness and width of the membrane, respectively, and R is the resistance value measured.

Methanol permeability was determined by using an H's cell. One side of the cell was filled with 2 M methanol, and the other side was filled with deionized water while the membrane was placed in the middle to separate the two sides. Magnetic stirrers were used in each compartment to ensure uniformity. The concentration of methanol was measured by a Shimadzu GC-1020A series gas chromatograph. The methanol diffusion coefficients were calculated from Equation (4):

$$C_B(t) = \frac{A}{V_B}\cdot\frac{DK}{L}\cdot C_A\cdot(t - t_0) \quad (4)$$

Where C_A is the methanol concentration of the feed side and C_B is the concentration that permeated through the membrane. A, L and V_B are the effective area, the thickness of the membrane and the volume of permeated compartment, respectively. DK is defined as the methanol permeability and t_0 is the time lag.

For the simulated polymer cell of SPP-*co*-PAEK CN *x* and SPP-*co*-PAEK MO *x* shown in Fig. 7, the molecular simulation was performed using the Material Studio software package (Accelrys Inc, CA, USA). For simulation, the commercial force field COMPASS was used. SPP-*co*-PAEK CN *x* and SPP-*co*-PAEK MO *x* chains with 20 repeat units were built and amorphous models were constructed at

Table 2
The IEC values, water uptake and swelling ratio of SPP-*co*-PAEK membranes.

Sample	IEC (mequiv g^{-1})		Water uptake (%)[b]	Swelling ratio (%)[c]	
	Theoretical	Experimental[a]		ΔT_c	ΔL_c
SPP-*co*-PAEK CN 4.00	2.59	2.54	77.0	21.3	18.2
SPP-*co*-PAEK CN 2.33	2.12	2.10	56.2	17.5	16.8
SPP-*co*-PAEK CN 1.86	1.90	1.87	43.0	12.9	10.0
SPP-*co*-PAEK MO 2.33	2.17	2.12	80.2	27.2	20.1
Nafion®117	–	0.91	33.8	23.7	24.0

[a] IEC by titration.
[b] At 80 °C.
[c] At 80 °C.

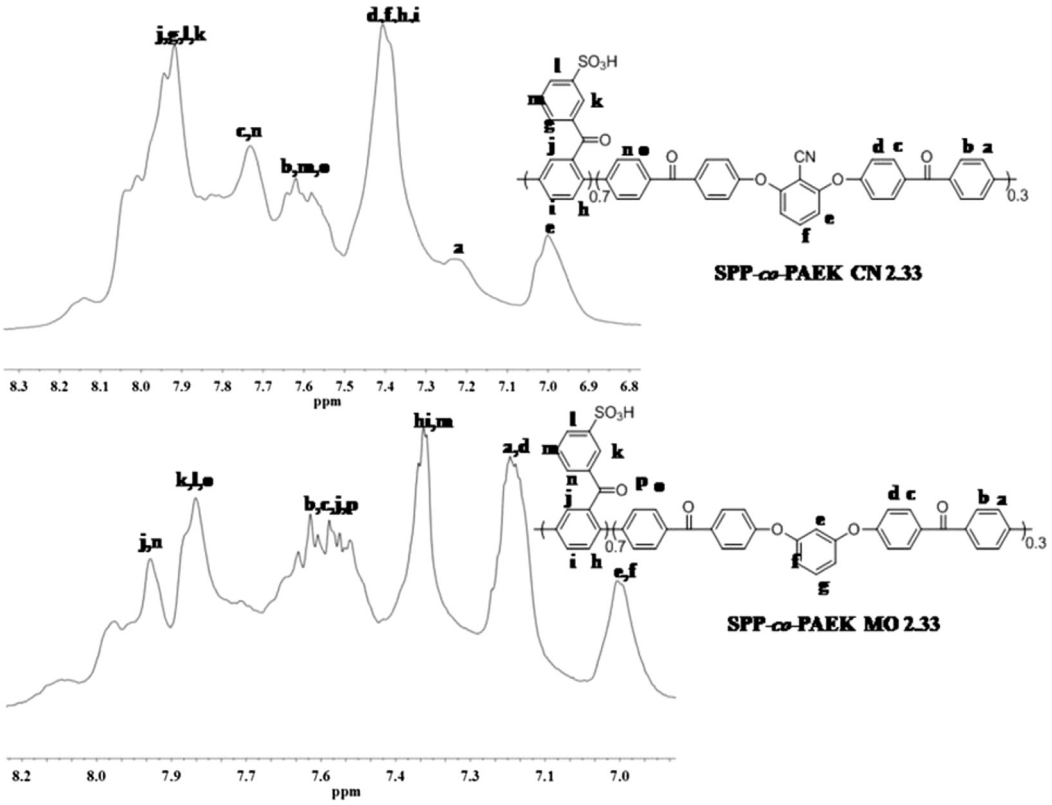

Fig. 3. ^{1}H NMR spectra of SPP-*co*-PAEK CN 2.33 and SPP-*co*-PAEK MO 2.33.

298 K under periodic boundary conditions using Amorphous Cell module in Material Studio 4.2. Successive iterations of energy-minimization and molecular dynamics (MD) simulations were performed using a time step of 1.0 fs for equilibrating the cells and obtaining the final densities. The hydrogen bonds were automatically detected using a hydrogen bond search program in a 3D atomistic periodic box. The calculated bond energy ranges from 1 kcal mol^{-1} to 5 kcal mol^{-1}.

A membrane-electrode assembly was fabricated according to the literature method [24,25]. A slurry which consisted of Vulcan XC-72 carbon and PTFE (20 wt. %) was coated onto the carbon paper (TGPH060, 20 wt. % PTFE, Toray) to form the cathode diffusion layer. The XC-72 carbon loading was kept at ca. 2 mg cm^{-2}. The anode diffusion layer was fabricated in the same way with ca. 2 mg cm^{-2} XC-72 carbon loading. The anode and cathode catalysts used in this work were Pt–Ru black with an atomic ratio 1:1 (HiSpec 6000, Johnson Matthey) and carbon-supported Pt with a Pt loading of 60 wt.% (HiSpec 9000, Johnson Matthey), respectively. Catalyst ink was prepared by dispersing appropriate amount of catalyst and 5 wt. % Nafion solutions (Aldrich) into a mixture of isopropyl alcohol and ultrapure water with a volume ratio of 1:1. The catalyst ink was then sprayed on the MPL. The metal loading was 4.0 ± 0.2 mg cm^{-2} for both cathode and anode, and the ionomer loading was 20 wt.% for the cathode and 15 wt.% for the anode, respectively. The MEA was fabricated by hot-pressing the anode and cathode onto the pretreated Nafion@117 membrane at 6 MPa and 170 °C for 3 min. The MEA performance was evaluated in a single cell with an active cross-section area of 4 cm^{2}. The MEA was immersed into 4 M methanol solution before the test. The polarization curves of the passive DMFCs under air-breathing mode were obtained on an Arbin FCT testing system (Arbin Instrument Inc. USA) by using 4 M methanol solution. For each discharging current point along the polarization curve, a 2 min waiting period was kept to obtain a stable voltage reading.

3. Results and discussion

3.1. Synthesis and characterization

Monomers **1** and **2** were simply synthesized via the aromatic nucleophilic substitution reactions with a high yield (>90%) as

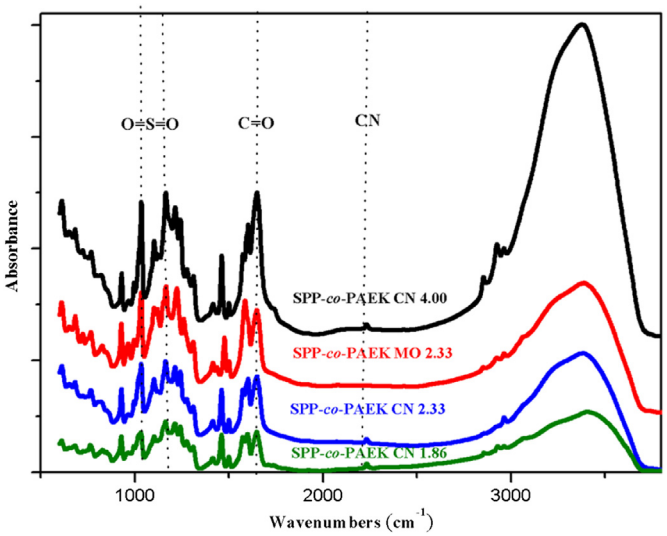

Fig. 4. FT-IR spectra of SPP-*co*-PAEK copolymers.

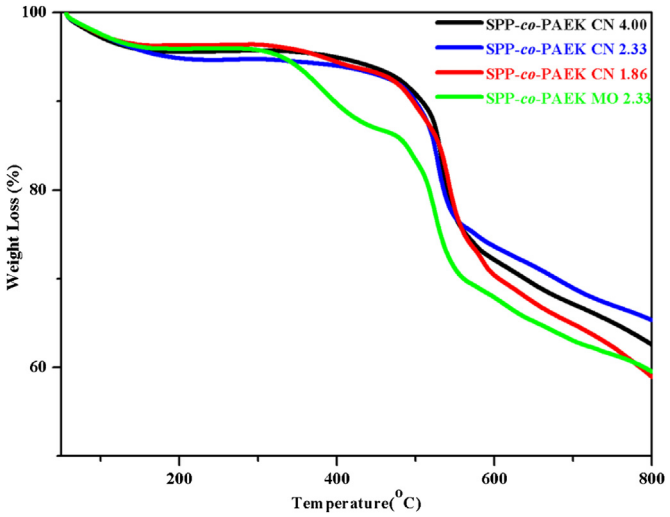

Fig. 5. TGA curves of SPP-*co*-PAEK membranes under N_2 atmosphere.

illustrated in Scheme 1. The chemical structures of the monomers were confirmed by ^{1}H NMR and ^{13}C NMR. All the peaks were assigned to the protons as designated in Fig. 2. The SPP-*co*-PAEK copolymers were prepared as illustrated in Scheme 2. The viscosity values of the obtained copolymers were 1.08–1.36 dL g^{-1}, as shown in Table 1. The polymerization yields were almost 100% and the measured IEC values were slightly (less than 2%) smaller than the calculated values (Table 2). These results indicate that the polymerizations were carried out successfully. The ^{1}H NMR spectra of SPP-*co*-PAEK copolymers are shown in Fig. 3, the positions of the peaks are consistent with the chemical structure of the copolymers. The FT-IR spectra of SPP-*co*-PAEK copolymers are shown in Fig. 4. The bands at 1660 cm^{-1} can be assigned to the stretching vibration of –C=O. The bands around 1097 cm^{-1} and 1028 cm^{-1} corresponds to the asymmetric and symmetric stretching bands of sulfonic acid groups, while the bands at 2250 cm^{-1} can be assigned to –CN groups. All copolymers were soluble in polar organic solvents such as DMAc, DMF, NMP and DMSO, and formed flexible and transparent membranes.

3.2. Thermal and mechanical properties

Fig. 5 shows the thermal stability of the copolymers investigated by TGA. The first weight loss starting from 200 to 300 °C can be ascribed to the decomposition of sulfonic acid groups by the desulfonation, while the second stage weight loss around 500 °C can be assigned to the decomposition of the polymer main chain. These results suggested the good thermo-stability of SPP-*co*-PAEK membranes. Moreover, the SPP-*co*-PAEK CN membranes showed no more than 10% weight loss before 500 °C. This can be attributed to strong hydrogen bonding interactions between polymer chains formed by cyano groups and other polar groups [26,27].

Mechanical properties of these SPP-*co*-PAEK membranes are shown in Table 1 and values of two SPP derivative membranes SPP-70 and F-SPPI-50 that our group reported before have been added for comparison [16,17]. When compared with SPP-70 and F-SPPI-50, these SPP-*co*-PAEK membranes exhibited a higher elongation ratio. Hence for practical applications, the obtained SPP-*co*-PAEK membranes could undergo fairly large deformation without breaking, especially during the process of MEA preparation.

Dynamic mechanical analysis (DMA) was used to determine the Tg values of the SPP-*co*-PAEK copolymers. As shown in Table 3, the glass-transition temperature of the SPP-*co*-PAEK CN 1.86 is 232 °C which was significantly lower than that of SPP-70 [16] (Tg > 500 °C). This shows that introducing a flexible unit into the main chain of the SPPs could significantly lower their Tg. Moreover, the unique *meta* linkage in the polymer main chain is also an important factor leading to the low Tg of SPP-*co*-PAEK copolymers. As we know, the *meta* linkage in the ether segment could also lower the Tg of the polymers because the angular shape of the meta linkage facilitates the movement of polymer chains more than the para linkage [22]. In addition, the SPP-*co*-PAEK polymers with ordered Tg can be easily prepared by adjusting the feed ratio of monomers as given in Table 3.

3.3. Water uptake and swelling ratio

Water uptake (WU) is closely related to the IEC values and the proton conductivity of PEMs, so it plays a dominant role in evaluating the final performance of PEMs. Existence of water molecules in the sulfonated membranes is expected to be beneficial for proton transport. However, over absorption of water can destroy the dimensional stability of membranes and the resulting swelling decreases the mechanical properties dramatically [28]. WUs of all the SPP-*co*-PAEK membranes were evaluated and the results are shown in Table 2 and Fig. 6. All the SPP-*co*-PAEK membranes showed increase in water absorption with the increase of the test temperature. Moreover, the water uptake values of the SPP-*co*-PAEK membranes increased with the increase of IEC values. However, it was interesting to observe that at high temperature (above 60 °C), the water uptake values of the SPP-*co*-PAEK MO 2.33 obviously exceeded that for SPP-*co*-PAEK CN 4.00. The swelling ratios of the membranes at 80 °C are shown in Table 2. Clearly, they have the same changing trends with WU results. All the SPP-*co*-PAEK membranes were observed to have lower swelling ratio than Nafion®117. For example, despite its IEC value of 1.86 mequiv g^{-1},

Table 3
Methanol permeability, proton conductivity and oxidative stability of SPP-*co*-PAEK copolymer membranes.

Sample	Tg (°C)	Proton conductivity S cm^{-1} (30 °C)	Methanol permeability[a] (cm^2 s^{-1}) 10^{-6}	Selectivity (S s cm^{-3}) 10^4	Oxidative stability	
					ζ_1 (h)[b]	ζ_2 (h)[b]
SPP-*co*-PAEK CN 4.00	–	0.072	0.76	9.54	11	64
SPP-*co*-PAEK CN 2.33	199.5	0.059	0.35	16.98	16	103
SPP-*co*-PAEK CN 1.86	232.0	0.038	0.23	16.70	22	146
SPP-*co*-PAEK MO 2.33	192.6	0.062	0.72	8.61	9	27
SPP-70[c]	>500	0.17	0.73	23.28	37	71
F-SPPI-50[c]	–	0.065	0.31	19.40	52	263
Nafion®117		0.090	2.4	3.75	–	–

[a] Measured at 25 °C.
[b] ζ_1 and ζ_2 refer to the elapsed times at which the membranes started to dissolve and dissolved completely in the solution (30% H_2O_2 aqueous solution containing 30 ppm $FeSO_4$) at 25 °C, respectively.
[c] Previously synthesized and added for comparison [16,17].

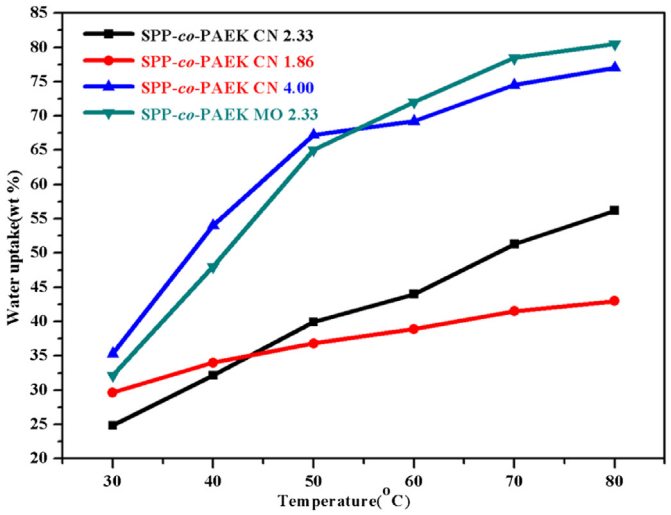

Fig. 6. Temperature dependence of water uptake of SPP-*co*-PAEK membranes.

the swelling ratio of SPP-*co*-PAEK CN 1.86 was 10%. A lower degree of swelling suggests that the SPP-*co*-PAEK membranes are more suitable for further applications. In addition, all SPP-*co*-PAEK CN membranes exhibited lower swelling ratio than SPP-*co*-PAEK MO 2.33 membrane. These results can be explained by the existence of abundant polar −CN groups in the polymer backbone. The strong interactions or hydrogen bonds between −CN and other polar groups, obviously restricts the dimensional change of the membranes, thus resulting in the decrease of WU values of SPP-*co*-PAEK CN *x*. Conformational analysis of SPP-*co*-PAEK MO *x* and SPP-*co*-PAEK CN *x* was modeled to further understand the effect of −CN groups in the polymer backbones. As shown in Fig. 7, strong intermolecular forces are present in SPP-*co*-PAEK CN *x* copolymers formed by the interaction of cyano groups with water molecules and sulfonate groups.

3.4. Morphology of membranes and proton conductivity

TEM images of SPP-*co*-PAEK membranes are shown in Fig. 8.The dark regions are representative of hydrophilic domains (ionic clusters) which is formed by Pb^{2+} staining, and the light regions represent the hydrophobic polymer backbone. The images show clear micro phase-separated structures comprising hydrophilic domains and hydrophobic moieties. The sulfonic acid groups in the present study are localized on the benzoyl side chains, which promotes the sulfonic acid groups to move together to form ion-rich channels. As clearly seen in Fig. 8, the distribution of the ion channels in these membranes became more and more intense as their IECs increasing.

Proton conductivity of the membranes is closely related to their morphology. Proton conductivity is a key transport property which directly determines the fuel cell performance. The proton conductivities of SPP-*co*-PAEK membranes and Nafion®117 were measured in water in the temperature range of 30–80 °C. As shown in Fig. 9, the proton conductivities of SPP-*co*-PAEK membranes are in the range of 0.038–0.073 S cm^{-1} at 30 °C, and the proton conductivity and WU have the same changing trend as the temperature changing. Moreover, the proton conductivities of SPP-*co*-PAEK CN membranes constantly increased with their IECs increasing over all the temperature ranges. This indicates that the IEC value is the dominant factor in determining the proton conductivities of SPP-*co*-PAEK membranes. Though the WUs of SPP-*co*-PAEK CN 2.33 are extremely low as compared to that of SPP-*co*-PAEK MO 2.33 within the test temperature range, their conductivities are very similar.

3.5. Oxidative stability and methanol permeation

The oxidative stability of the membranes was investigated by observing their dissolving behavior in Fenton's reagent (30% H_2O_2 solution containing 30 ppm $FeSO_4$) at 25 °C. As shown in Table 3, we can find that SPP-*co*-PAEK CN 1.86 exhibited the best oxidative stability among all the SPP-*co*-PAEK membrane. SPP-*co*-PAEK CN 1.86 endured 22 h before it started to dissolve and it took 146 h to dissolve completely. In addition, the SPP-*co*-PAEK CN 4.00 membrane and SPP-*co*-PAEK CN 2.33 membrane were stable upto 11 and 16 h respectively and they dissolved completely after 64 and 103 h respectively. In comparison, SPP-*co*-PAEK MO 2.33 membrane could not endure more than 9 h after which it started dissolving in the oxidizing solution. A reasonable concordance was observed between the results of the oxidative stability and the swelling ratio. The degradation of the membrane during the operation of the cell is usually believed to be a combination of chemical, thermal, and mechanical effects. The greater swelling of membranes can cause defects or pinholes in the membrane and thus accelerate the

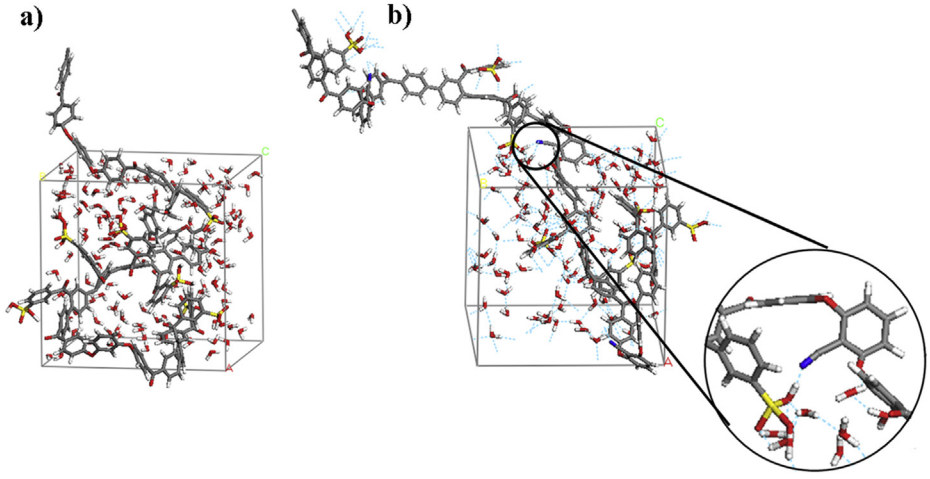

Fig. 7. a) Three-dimensional view of SPP-*co*-PAEK MO *x* in an amorphous periodic cell (the number of repeat unit in SPP-*co*-PAEK MO *x* is 20), b) Three-dimensional view of SPP-*co*-PAEK CN *x* in an amorphous periodic cell (the number of repeat unit in SPP-*co*-PAEK CN *x* is 20), the blue dots represent cyano groups. (For interpretation of the references to color in this figure legend, the reader is referred to the web version of this article.)

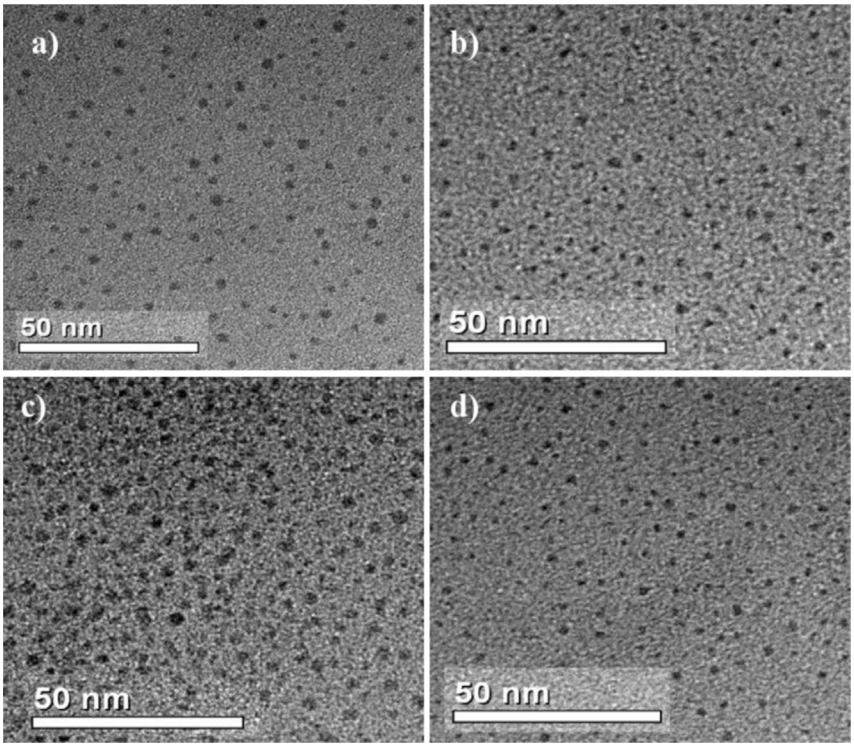

Fig. 8. TEM images of a) SPP-*co*-PAEK CN 1.86 b) SPP-*co*-PAEK CN 2.33 c) SPP-*co*-PAEK CN 4.00 d) SPP-*co*-PAEK MO 2.33.

oxidative degradation of the membrane [29]. Moreover, the oxidative stabilities of SPP-*co*-PAEK are much lower than SPP-70 and F-SPPI-50. This could possibly be due to the much higher electron densities of SPP-*co*-PAEK copolymers than SPP-70 and F-SPPI-50 resulting from the introduction of ether bonds into their main chains. Hence the electrophilic attack was accelerated during the oxidative stability test [30]. In addition, through an accelerated test, the oxidative stability of the SPP-*co*-PAEK membranes was still proved to be much better than most sulfonated aromatic polymers reported before [31–35]. During this test, film samples were soaked in Fenton's reagent (3% H_2O_2 solution containing 2 ppm $FeSO_4$) at 80 °C for 1 h and the weight change of the films was recorded. After the test, the mechanical properties of the SPP-*co*-PAEK membranes were still maintained and over 99% of the initial weights of the films were retained. In general, the Tg values of SPP-*co*-PAEK copolymers are much lower than the SPPs, and their oxidative stability is superior when compared with other SAPs.

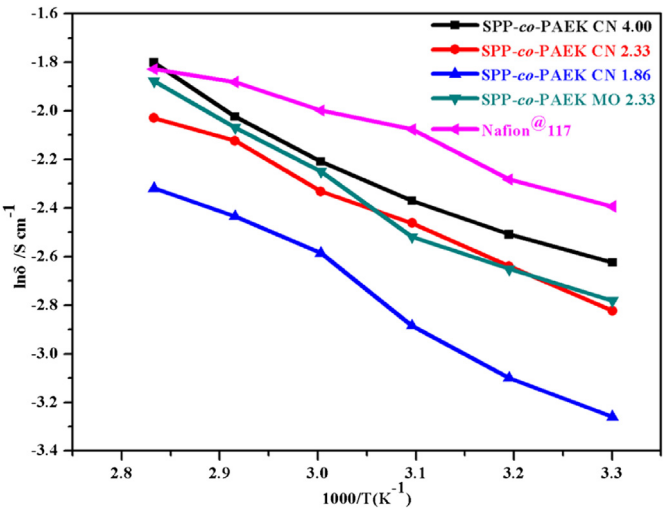

Fig. 9. Arrhenius plots under 100% RH environment for SPP-*co*-PAEK membranes and Nafion@117.

Methanol permeation is a key parameter in determining the DMFC performances. High methanol permeation will decrease the efficiency of the DMFCs. As shown in Table 3, the SPP-*co*-PAEK membranes possessed low methanol permeability at room temperature, with values in the range of 0.23×10^{-6} to 0.76×10^{-6} $cm^2\ S^{-1}$, which is lower than the value of Nafion@117 (2.40×10^{-6} $cm^2\ S^{-1}$). The selectivity, which is the ratio of proton conductivity (σ) to methanol permeability (P), was also used to estimate the membrane performance. The selectivity of the SPP-*co*-PAEK membranes were all higher than that of Nafion@117. These results showed that all the SPP-*co*-PAEK membranes were suitable for DMFC applications.

3.6. Single-cell performance

As discussed above, the prepared SPP-*co*-PAEK membranes showed the good mechanical property, oxidative stability, low methanol permeation and good proton conductivity. Therefore, MEAs were fabricated with these membranes respectively and then evaluated by the electrochemical performance. The fuel cell was operated at 25 °C with the supply of 4 M methanol to anode and air to cathode. Fig. 10 showed the single cell performance of DMFCs comprising Nafion@117 membrane and SPP-*co*-PAEK membranes as polymer electrolytes, including the polarization and power density as a function of the current density. As we can see, the fuel cell with SPP-*co*-PAEK CN 1.86 membrane had a max power density 24.5 mW cm^{-2} which was comparable to the value of Nafion@117 (24.3 mW cm^{-1}) under the same operating conditions. The high performance of SPP-*co*-PAEK CN 1.86 membrane could be attributed to its much higher selective factor. The optimization of the catalysts and the MEA fabrication procedure is our next project.

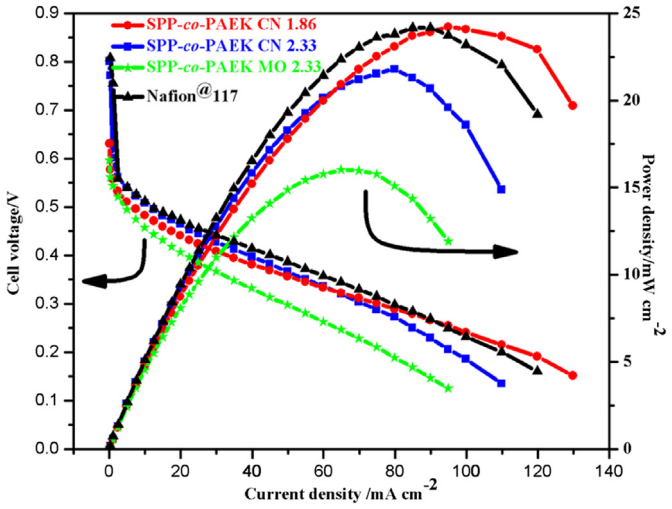

Fig. 10. Performance of DMFCs with Nafion@117 and SPP-*co*-PAEK copolymers membranes at 25 °C under air-breathing mode with supply with 4 M methanol solution.

4. Conclusions

In summary, a new series of SPP-*co*-PAEK copolymers were prepared from SBJT and **1** or **2** through nickel (0) catalytic coupling copolymerization, respectively. These membranes all showed good mechanical property, low methanol permeation. Moreover, SPP-*co*-PAEK CN membranes exhibited comparable oxidative stability with other sulfonated polyphenylenes derivatives we mentioned before, such as SPP-70 and F-SPPI-50. In addition, the cast membranes all formed well-defined micro-phase separation structure which was favorable for proton transport. Furthermore, by introducing flexible units into rigid main chain of SPPs, SPP-*co*-PAEK membranes showed preferable cell compatibility. That means it is easier to make MEAs with these membranes by hot-pressing method. Then, the cell performance of the SPP-*co*-PAEK membranes was tested, and SPP-*co*-PAEK CN 1.86 showed a higher max power density than Nafion@117 when performing under the same conditions. All the results revealed that these novel SPP-*co*-PAEK copolymers could be the promising PEM materials for DMFCs applications.

Acknowledgments

We thank the National Basic Research Program of China (No. 2012CB932802), the National Science Foundation of China (No. 51021003, 51133008, 21074133, 21304092), the National High Technology Research and Development Program of China (863 Program) (No. 2012AA03A601) for financial support.

References

[1] L. Fu, G. Xiao, D. Yan, J. Mater. Chem. 22 (2012) 13714–13722.
[2] M.A. Hicker, H. Ghassemi, Y.S. Kim, B.R. Einsla, J.E. McGrath, Chem. Rev. 104 (2004) 4587–4612.
[3] C.H. Paek, C.H. Lee, M.D. Guiver, Y.M. Lee, Prog. Polym. Sci. 36 (2011) 1443–1498.
[4] B.C.H. Steele, A. Heinzel, Nature 414 (2001) 345.
[5] X. Guo, J. Fang, T. Watari, K. Tanaka, H. Kita, K. Okamoto, Macromolecules 35 (2002) 6707–6713.
[6] J. Pang, H. Zhang, X. Li, Z. Jiang, Macromolecules 40 (2007) 9435–9442.
[7] S. Tian, D. Shu, S. Wang, M. Xiao, Y. Meng, J. Power Sources 224 (2013) 42–49.
[8] Y. Lin, Polym. Chem. 3 (2012) 1373.
[9] N. Carretta, V. Tricoli, F. Picchioni, J. Membr. Sci. 166 (2000) 189–197.
[10] T. Nakagawa, K. Nakabayashi, T. Higashihara, M. Ueda, J. Mater. Sci. 20 (2010) 6662–6667.
[11] X. Zhang, L. Sheng, T. Higashihara, M. Ueda, Polym. Chem. 4 (2013) 1235–1242.
[12] S. Seesukphronrarak, K. Ohira, K. Kidena, N. Takimoto, C.S. Kuroda, A. Ohira, Polymer 51 (2010) 623–631.
[13] K. Umezawa, T. Oshima, M. Yoshizawa-Fujita, Y. Takeoka, M. Rikukawa, ACS Macro Lett. 1 (2012) 969–972.
[14] X. Zhang, Z. Hu, L. Luo, S. Chen, J. Liu, S. Chen, L. Wang, Macromol. Rapid Commun. 32 (2011) 1108.
[15] K. Si, D. Dong, R. Wycisk, M. Litt, J. Mater. Chem. 22 (2012) 20907.
[16] S. Wu, Z. Qiu, S. Zhang, X. Yang, F. Yang, Z. Li, Polymer 47 (2006) 6993–7000.
[17] Z. Qiu, S. Wu, Z. Li, S. Zhang, W. Xing, C. Liu, Macromolecules 39 (2006) 6425–6432.
[18] H. Ghassemi, J.E. McGrath, Polymer 45 (2004) 5847–5854.
[19] X. Zhang, S. Chen, J. Liu, Z. Hu, S. Chen, L. Wang, J. Membr. Sci. 371 (2011) 276–285.
[20] X. Zhang, Z. Hu, Y. Pu, S. Chen, J. Ling, H. Bi, S. Chen, L. Wang, K. Okamato, J. Power Sources 216 (2012) 261–268.
[21] Y. Sakaguchi, K. Kitamura, M. Yamashita, S. Takase, K. Takasugi, Y. Akitomo, Macromolecules 45 (2012) 5403–5409.
[22] X. Li, F.P.V. Paoloni, E.A. Weiber, Z. Jiang, P. Jannasch, Macromolecules 45 (2012) 1447–1459.
[23] S. Ushijima, S. Dohi, K. Moriyama, H. Togo, Tetrahedron 68 (2012) 1436–1442.
[24] M. Chen, J. Chen, Y. Li, Q. Huang, H. Zhang, X. Xue, Z. Zou, H. Yang, Energy Fuels 26 (2012) 1178–1184.
[25] M. Chen, S. Wang, Z. Zou, T. Yuan, Z. Li, D. Akins, H. Yang, J. Appl. Electrochem. 40 (2010) 2117–2124.
[26] Y. Song, Y. Jin, Q. Liang, K. Li, Y. Zhang, W. Hu, Z. Jiang, B. Liu, J. Power Sources 238 (2013) 236–244.
[27] R. Langner, G. Zundel, J. Phys. Chem. 99 (1995) 12214–12219.
[28] B. Bae, T. Yoda, K. Miyatake, H. Uchida, M. Watanade, Angew. Chem. Int. Ed. 49 (2010) 317–320.
[29] A. Kusoglu, A.M. Karlsson, M.H. Santare, S. Cleghom, W.B. Johnson, J. Power Sources 161 (2006) 987–996.
[30] H. Ghassemi, J.E. McGrath, T.A. Zawodzinski, Polymer 47 (2006) 4132–4139.
[31] D. Shin, S. Lee, N. Kang, K. Lee, M.D. Guiver, Y. Lee, Macromolecules 46 (2013) 3452–3460.
[32] H. Liao, G. Xiao, D. Yan, Chem. Commun. 49 (2013) 3979–3981.
[33] N. Tan, G. Xiao, D. Yan, Chem. Mater. 22 (2010) 1022–1031.
[34] S. Tian, D. Shu, S. Wang, M. Xiao, Y. Meng, Fuel Cells 3 (2007) 232–237.
[35] D. Gomes, J. Roeder, M.L. Ponce, S.P. Nunes, J. Power Sources 175 (2008) 49–59.